

Ab-Initio Calculation of the Electrical Conductivity, Optical Absorption, and Reflectivity of the 2D Materials SnC and NbC

Nadxieli Delgado ¹, Osiris Salas ², Erick Garcés ³ and Luis Fernando Magaña ^{1,*} 

¹ Instituto de Física, Universidad Nacional Autónoma de México, Apartado Postal 20-364, Mexico City 01000, Mexico

² Instituto Politécnico Nacional, Escuela Superior de Ingeniería Mecánica y Eléctrica, Avenida Instituto Politécnico Nacional, S/N, Mexico City 07340, Mexico

³ Tecnológico Nacional de México, Tecnológico de Estudios Superiores de Ixtapaluca, Km. 7 Carretera Ixtapaluca-Coatepec, San Juan Coatepec, Ixtapaluca 56580, Mexico

* Correspondence: fernando@fisica.unam.mx

Abstract: Using density functional theory (DFT), we performed first-principles calculations of the electrical conductivity, optical absorption, and reflectivity for the 2D carbides SnC and NbC. We calculated the electronic energy band structure of the materials. We performed the calculations without considering the spin-orbit coupling (SOC) term and including it. We determined that 2D SnC is a semiconductor material and 2D NbC is a conductor. We compared the optical absorption and reflectivity with those of graphene. We found that the 2D SnC and graphene optical absorptions in the infrared region are similar and small; the corresponding values for 2D NbC are approximately ten times larger. In the visible range, the absorption values for 2D SnC and 2D NbC are of the same magnitude and much more significant than graphene. We found that the 2D NbC optical absorption for the ultraviolet region was close to zero. Graphene and 2D SnC have similar maximum values for absorption but at different energies. We determined that graphene reflectivity is larger but similar to that of 2D NbC, and that the 2D SnC reflectivity is near zero. Finally, the 2D NbC electrical conductivity value was about ten times larger than the corresponding value for 2D SnC. As expected, when there was a change of dimensionality, the related 3D materials showed a vastly different value for the electrical conductivity. The 2D materials showed conductivities significantly smaller than those of 3D materials in both cases. The results we obtained for 2D SnC and 2D NbC when we included the SOC term showed that the electrical conductivity for 2D SnC increased by 13.18% and 2D NbC by 18.16%. The optical properties changed, particularly the location of the peaks in the optical absorption and reflectivity.

Keywords: 2D materials; 2D SnC; 2D NbC; optical properties; electrical conductivity



Citation: Delgado, N.; Salas, O.; Garcés, E.; Magaña, L.F. Ab-Initio Calculation of the Electrical Conductivity, Optical Absorption, and Reflectivity of the 2D Materials SnC and NbC. *Crystals* **2023**, *13*, 682. <https://doi.org/10.3390/cryst13040682>

Academic Editor: Andreas Thissen

Received: 7 March 2023

Revised: 10 April 2023

Accepted: 14 April 2023

Published: 16 April 2023



Copyright: © 2023 by the authors. Licensee MDPI, Basel, Switzerland. This article is an open access article distributed under the terms and conditions of the Creative Commons Attribution (CC BY) license (<https://creativecommons.org/licenses/by/4.0/>).

1. Introduction

Transition metal carbides, such as NbC, are layered compounds and sources of 2D materials. These ceramic materials have high electrical and thermal conductivities, hardness, and melting points. Thus, they can be used for applications such as diffusion-resistant thin-film coatings of microcircuit devices, cutting and grinding tools, hard electrical contacts, and many more [1]. They exhibit a weak van der Waals bonding force between layers and a more substantial bonding force between atoms within a plane. We must mention that the 2D materials obtained from these compounds are not necessarily one-atom thick; many are three-atom thick materials. In the case of 2D NbC, we have a one-atom-thick material [2,3]. The powder form of 3D NbC is available on the market. Its crystal structure is cubic and isomorphic to the NaCl structure, with space group Fm3m; Number 225.

SnC is a compound formed by two group IV elements and there are practical difficulties in obtaining it. 3D SnC is also available on the market. Furthermore, its unusual properties are of particular research interest [4]. Theoretical investigations predict that

pristine 3D SnC is a semiconductor [5] and that 2D SnC is a stable, one-atom-thick material with a hexagonal structure belonging to the $P6\ m2$ -number 156 space group [6]. It is similar to boron nitride, graphene, and semiconductors [7]. Additionally, 2D SnC could be an anode material for lithium-ion or sodium-ion batteries [7,8]. Given that it is a 2D material, it easily supports strain, which is a convenient property to apply in spintronics and optoelectronics. Additionally, its enormous surface area is very appealing for applications as an anode.

The dimensionality may significantly influence the transport properties of materials. The number of degrees of freedom is significant for the particles' movement. Therefore, for the material's charge transport (electrical conductivity) and other properties, it is usual to observe a change in electrical conductivity when the dimensionality of a sample diminishes. An obvious example is the case of graphite and graphene. Exploring the properties of 2D materials is necessary to use them in practical applications. In this work, we investigated, from the first principles, the electrical conductivity, optical absorption, and reflectivity of SnC and NbC. We used density functional theory (DFT) within the generalized gradient approximation (GGA) with the Quantum ESPRESSO code [9]. We performed our ab-initio calculations in two ways: one without considering the spin-orbit coupling (SOC) term, and the other including it.

2. Materials and Methods

We performed first-principles calculations and obtained the electrical conductivity, the electronic energy band structure, and the optical absorption and reflectivity of the 2D materials SnC and NbC. We compared our results to each other and to graphene. We optimized the configuration of these materials using the Quantum ESPRESSO code [9] with density functional theory within the GGA approximation.

We used the Troullier–Martins pseudopotentials [10], which are norm-conserving, with the Perdew–Burke–Ernzerhof (PBE) approximation [11] for the (GGA) approximation. We calculated the electronic energy band structures with and without SOC to compare the resulting conductivities and optical properties. Notice that including SOC implies a fully relativistic calculation. Furthermore, we took 50 k points within the Monkhorst–Pack k point scheme [12] and a cut-off energy of 1000 eV. We chose 1.0×10^{-6} eV for the threshold value for convergence. We considered periodic boundary conditions, and for SnC, an initial unit cell (see Figure 1a) with $\mathbf{a} = \mathbf{b} = 3.551$ Å and $\mathbf{c} = 16$ Å. This value of \mathbf{c} is enough to avoid interactions between the surfaces of neighboring cells. Notice that we have two atoms in the unit cell (a carbon atom and a Sn atom). In the case of NbC, we took a unit cell with $\mathbf{a} = \mathbf{b} = 4.101$ Å and $\mathbf{c} = 16$ Å (see Figure 1b). In this case, we have four atoms in the unit cell, two Nb atoms, and two C atoms. Again, we took a significant value of \mathbf{c} to avoid spurious interactions. We obtained the corresponding bond lengths to validate our chosen pseudopotentials for C, Sn, and Nb. Thus, we found a C–C bond size of 1.419 Å for graphene and an experimental value of 1.421 Å [13], which agrees well with our result. In the case of Sn, the observed Sn–Sn bond length was 2.810 Å [13], in agreement with our calculation of 2.814 Å. In the case of Nb, the calculated bond length was 2.863 Å, which agrees with the experimental value of 2.858 Å [11]. From the random phase approximation [14], we obtained the dielectric tensor in the limit of the linear optics and the Kramers–Kronig relations [15]. Then, we obtained the absorption and reflectivity for each case, considering the electromagnetic wave with a propagation direction perpendicular to the surface. The reader may see the calculation procedure in [16].

We calculated the energy bands using the Wannier90 code [17] to obtain electrical conductivity. Afterward, to solve the semiclassical Boltzmann transport equations, we considered an infinite homogeneous system using a constant relaxation time [18].

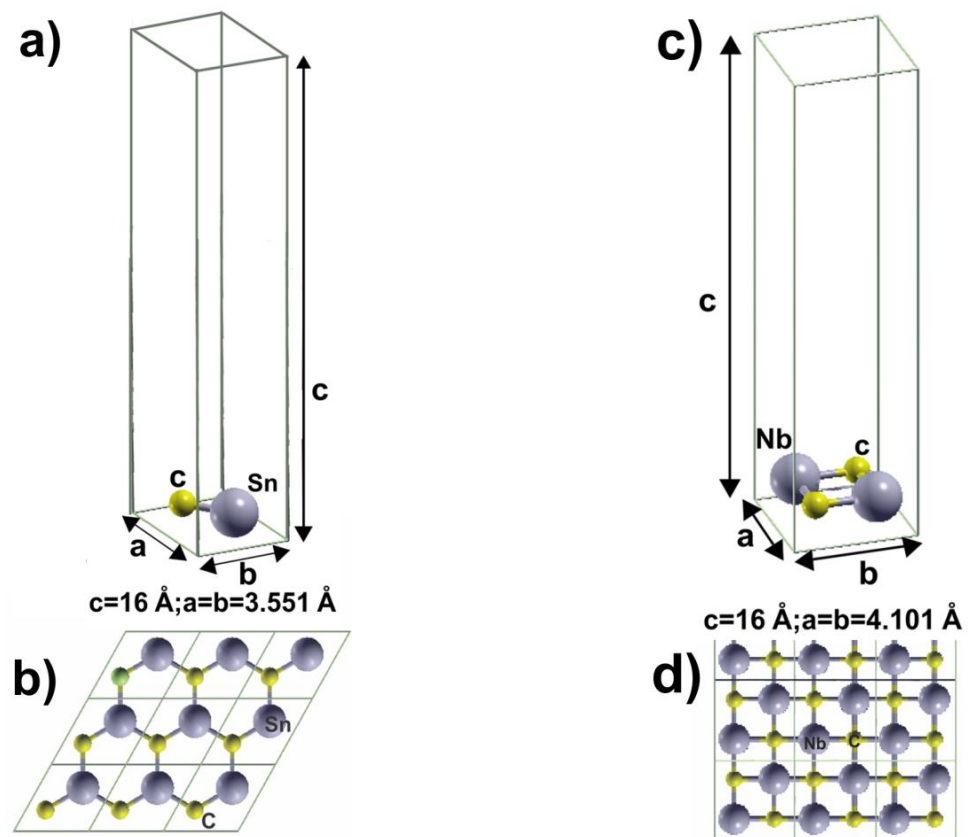


Figure 1. Result of our optimization for the 2D materials we considered. The unit cell for SnC (a); hexagonal symmetry of the surface for 2D SnC (b); the prediction for 2D SnC is a surface with a hexagonal lattice; the unit cell for monolayer 2D NbC (c); The optimization result for 2D NbC is a squared lattice (d).

3. Results

We optimized the configuration of these materials using the Quantum ESPRESSO code (Giannozzi et al., 2009) with density functional theory within the GGA approximation. The optimized lattice parameter we obtained for NbC (4.104 \AA) and the Nb-C bond distance (2.164 \AA) are in agreement with those reported in the literature (4.100 \AA , 2.15 \AA , respectively) [2]. Furthermore, in the case of SnC, we obtained, after optimization, 3.063 \AA for the lattice parameter and 2.062 \AA for the bond length of SnC, in agreement with the corresponding values reported in [19] (3.551 \AA and 2.051 \AA , respectively). We should mention that, given that there are experimental data for 2D NbC and that our results agree with those data, it is unnecessary to test the material's stability [3]. On the other hand, in the case of SnC, in Ref. [19], the authors predict and verify a 2D stable structure with lattice parameters that agree with our results. Thus, it is not necessary to test its stability. Subsequently, we calculated the electronic energy band structure, the electrical conductivity, and the optical absorption and reflectivity of the 2D materials SnC and NbC.

Figure 1a–d shows the optimized structures of the 2D materials SnC and NbC. Figure 2 presents the projected density of states (PDOS) for 2D SnC, which has a hexagonal symmetry. The results in Figure 2a do not include the SOC term. In Figure 2b,c, our calculations include SOC. Notice the gap around the Fermi energy in both cases; that implies this material is a semiconductor. In (b), we also show the total angular momentum $J = 2l - 1$ and $2l + 1$. We can notice the hybridization of orbitals s and p from carbon atoms with orbitals s and p from tin atoms below the Fermi energy. We have the same behavior above the Fermi energy. This hybridization is common in 2D materials such as, in this case, graphene and hBN.

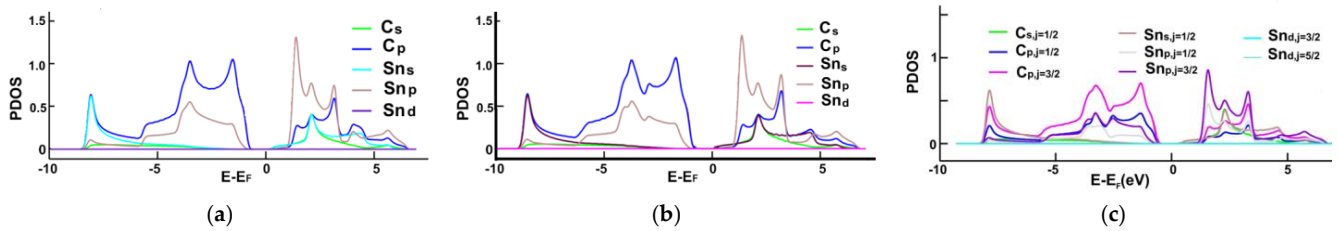


Figure 2. Projected density of states (PDOS) for 2D SnC. (a) The results without including the SOC term; (b,c) our results including SOC. Notice the gap around the Fermi energy in both cases. The material is a semiconductor. Furthermore, notice the hybridization of orbitals *s* and *p* from carbon atoms with orbitals *s* and *p* from tin atoms below and above the Fermi energy. This kind of hybridization is in graphene, and it is a typical feature of 2D materials with hexagonal symmetry, such as 2D SnC or 2d hBN. As we indicate in the energy band structure results, an indirect gap of 1.24 eV in (a) decreases to 1.07 eV in (b). In (b), we also show the total angular momentum $J = 2l - 1$ and $2l + 1$.

Figure 3 shows the PDOS for 2D NbC. In Figure 3a, we have a calculation without the SOC term. In Figure 3b,c, our results include the SOC. Notice that there is no gap around the Fermi energy in both cases. Thus, the material is a conductor. Notice the hybridization of orbitals *s* and *p* from carbon atoms with orbitals *s*, *p*, and *d* from niobium atoms below and above the Fermi energy. In Figure 3b, we also show the total angular momentum $J = 2l - 1$ and $2l + 1$. This hybridization differs from 2D SnC, where the *d* orbitals do not participate in the hybridization of the orbitals. The symmetry of 2D NbC is not hexagonal but cubic, and this symmetry originates different orbital hybridizations.

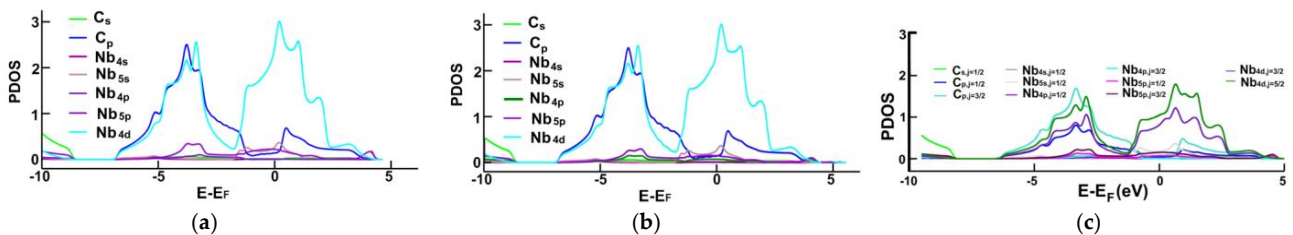


Figure 3. Projected density of states (PDOS) for 2D NbC. (a) A calculation without the SOC term. (b,c) Results include the SOC. In both cases, there is no gap around the Fermi energy. Thus, the material is a conductor. Notice the hybridization of orbitals *s* and *p* from carbon atoms with orbitals *s*, *p*, and *d* from niobium atoms below and above the Fermi energy. The symmetry of 2D NbC is not hexagonal, it is squared. In (b), we also show the total angular momentum $J = 2l - 1$ and $2l + 1$.

3.1. Energy Band Structures and Electrical Conductivities

Figures 4 and 5 show the energy band structures for SnC and NbC, respectively.

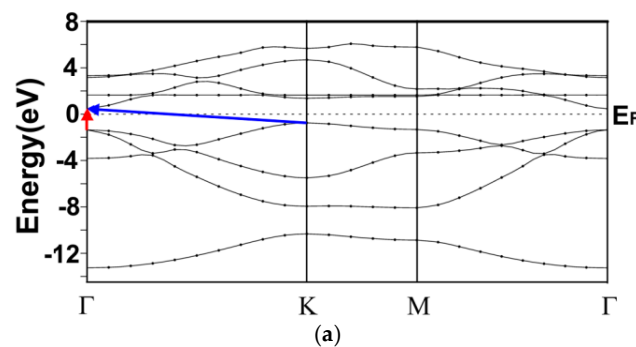


Figure 4. Cont.

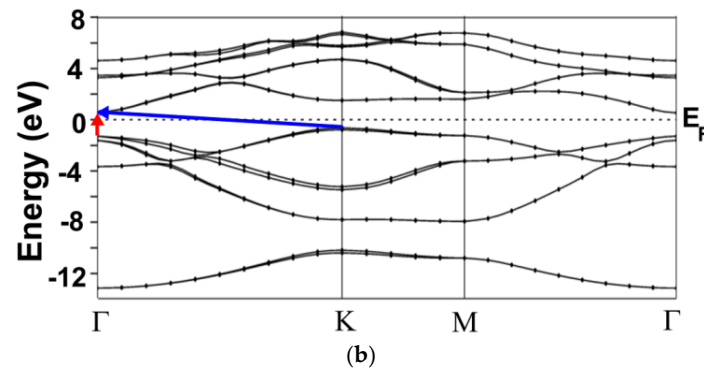


Figure 4. Electronic energy band structure for 2D SnC. (a) Result without SOC; (b) results with SOC. In both cases, there is a gap around the Fermi energy; thus, this material is a semiconductor. Notice the direct band gap at the Γ point (red arrow) of 1.77 eV in both cases and the smaller indirect gap (blue arrow) of 1.24 eV in (a) and 1.07 eV in (b).

Figure 4a shows the energy band structures for 2D SnC calculated without the SOC term. We can see a direct gap (red arrow) at the Γ point of 1.77 eV and an indirect gap of 1.24 eV, which we indicate with a blue arrow. Thus, this material is a semiconductor. Our results agree with those reported in [19].

Figure 4b shows the result we obtained for the energy band structure for 2D SnC considering the SOC term. There are some changes, in particular, above the Fermi energy. There were splittings in the energy levels, and the indirect band gap (blue arrow) decreased to 1.07 eV. The direct gap (red arrow) remained at 1.77 eV. Again, our results agree with those reported in [19].

The corresponding calculated electrical conductivity from the energy band structures was 1.00076×10^3 S/m without SOC and 1.01395×10^3 S/m with SOC. The difference in values for the conductivity implies an increase of 13.18%. We could not find an experimental or theoretical result for the conductivity in 2D SnC to compare with ours. Notice that the observed electrical conductivity value in 3D SnC was nearly ten times larger: 1.32×10^4 S/m. We expected the conductivity of 3D SnC to differ from 2D SnC due to the reduced degrees of freedom of the charge carriers in the material.

Figure 5a shows the electronic energy band structure for NbC without the SOC term, and Figure 5b includes it. Notice that the two cases have no band gap; this material is a conductor. There were few but essential changes in the band structure. In Figure 5b, we encircled the zone where the number of energy levels increased, and these levels cut and were very close to one that crossed the Fermi energy. This fact increases the value of electrical conductivity.

The calculated electrical conductivity for 2D NbC is 1.09530×10^4 S/m without SOC and 1.2942×10^4 with SOC; we obtained an increment of 18.16%. We could not find an experimental or theoretical value for 2D NbC to compare with our results; the corresponding observed value for 3D NbC is one hundred times larger: 1.35×10^6 S/m. Again, the conductivity of 3D NbC differs from 2D NbC, as expected.

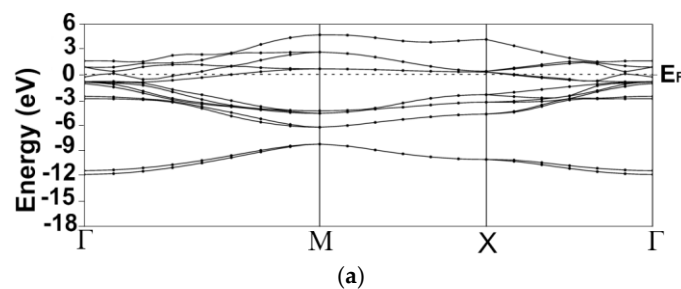


Figure 5. Cont.

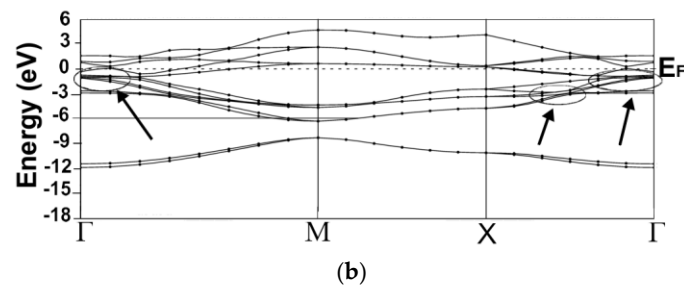


Figure 5. Electronic energy band structure for 2D NbC. (a) Result without SOC; (b) results with SOC. In both cases, there is no gap around the Fermi energy; thus, this material is a conductor. In (b), the encircled zone indicates where the number of energy levels increased, and these levels cut or were very close to one that crossed the Fermi energy. This fact increases the value of electrical conductivity.

3.2. Optical Properties

3.2.1. Absorption

Figures 6–8 compare the optical absorption of 2D SnC, 2D NbC, and graphene in the infrared, visible, and ultraviolet ranges.

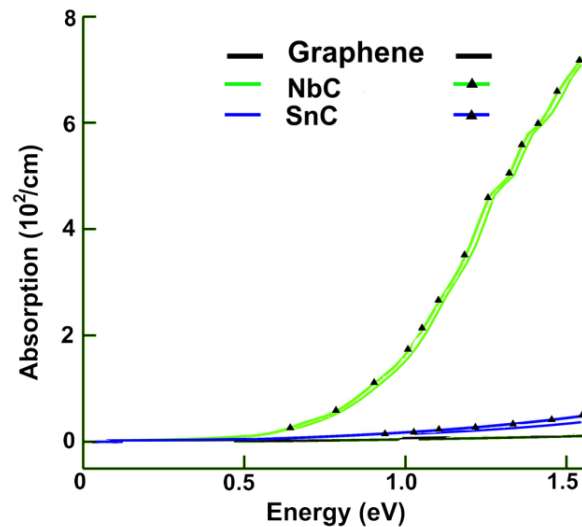


Figure 6. Comparison of the optical absorptions, in the infrared region, for the 2D materials SnC, NbC, and graphene. The solid triangles indicate our results obtained with the SOC term.

Figure 6 compares the optical absorptions for the 2D materials SnC, NbC, and graphene in the infrared region. We notice that the optical absorptions for 2D SnC and graphene were very similar. The absorption for 2D NbC was much larger. The solid triangles indicate our results obtained with the SOC term. In this region, the inclusion of SOC generated small changes.

Figure 7 compares the optical absorptions for the same 2D materials in the visible region. We notice that the optical absorptions for 2D SnC and 2D NbC were similar in this range, in contrast with the situation in the infrared region, due to their different energy band structures. The value for NbC was two or three times the value for SnC; however, the absorption for graphene was much smaller. The solid triangles indicate our results obtained with the SOC term. In this region, the inclusion of SOC generated more significant changes than in the infrared range.

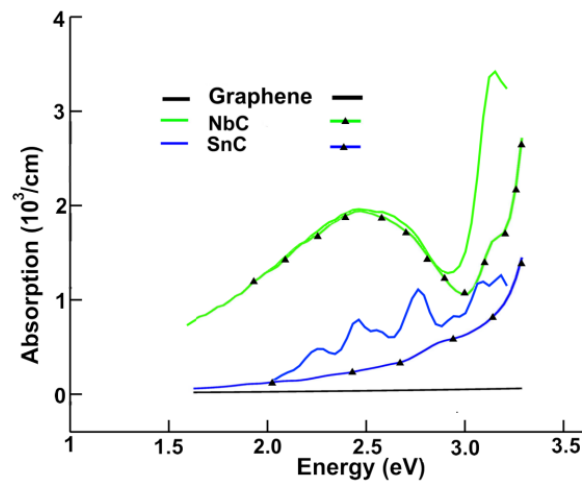


Figure 7. Comparison of the optical absorptions, in the visible range, for the 2D materials SnC, NbC, and graphene. The solid triangles indicate our results obtained with the SOC term.

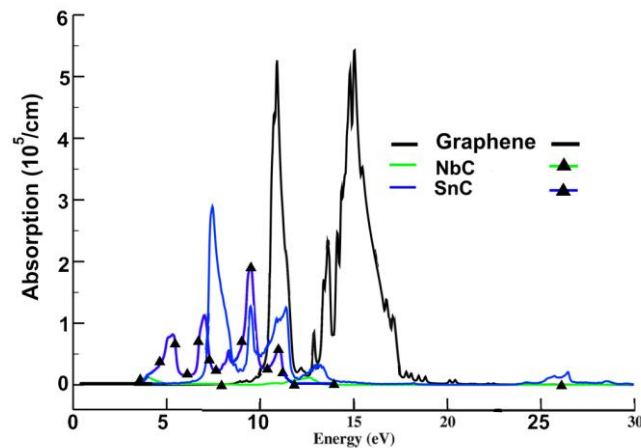


Figure 8. Comparison of the optical absorptions, in the ultraviolet range, for the 2D materials SnC, NbC, and graphene. The solid triangles indicate our results obtained with the SOC term.

The several peaks appearing for SnC came from the possible transitions from level-to-level present in the electronic energy band structure for SnC, which were smaller in number than those for NbC. Notice that the number of energy levels increased when we included SOC in the band structure calculation, and the curve smoothed.

Figure 8 compares the optical absorption of the same three 2D materials in the ultraviolet range. Notice that the optical absorption of NbC was nearly zero, in high contrast with what happened in the infrared region, due again to their different energy band structures. The absorptions of SnC and graphene have similar magnitudes, but the peaks were at different energies. The solid triangles indicate our results obtained with the SOC term. In this region, the inclusion of SOC generated more significant changes than in the infrared and visible ranges.

3.2.2. Reflectivity

Finally, Figure 9 compares the reflectivities of the same three 2D materials. The reflectivity of NbC was nearly zero. The reflectivities of SnC and graphene had similar magnitudes, but the peaks were at different energies. Including SOC generated significant changes for SnC, and NbC did not change and remained very small.

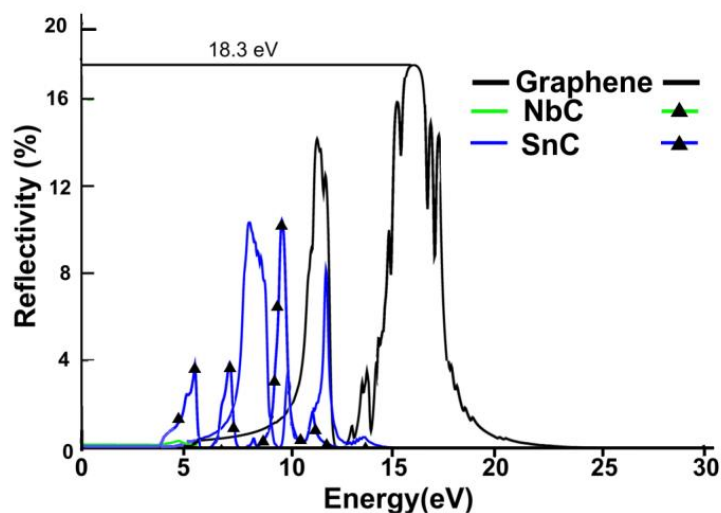


Figure 9. Comparison of the reflectivities for the 2D materials SnC, NbC, and graphene. The solid triangles indicate our results obtained with the SOC term.

4. Discussion

We used DFT to perform first-principles calculations of the electronic properties of the 2D carbides SnC and NbC. We obtained these materials' electronic energy band structure and found that 2D SnC is a semiconductor material, and 2D NbC is a conductor. We also found the electrical conductivity of the 2D SnC to be 1.00076×10^3 S/m without SOC and 1.01395×10^3 S/m with SOC. The difference in values for the conductivity implies an increase of 13.18%. These calculated values are smaller than the corresponding reported experimental values for the 3D SnC (1.32×10^4 S/m). For 2D NbC, the conductivity is 1.09530×10^4 S/m without SOC and 1.2942×10^4 with SOC; we obtained an increment of 18.16%. The corresponding observed value for 3D NbC is one hundred times larger: 1.35×10^6 S/m. We could not find experimental or theoretical values for 2D SnC or 2D NbC to compare with our results.

On the other hand, in the infrared region, the SnC and graphene optical absorptions are similar and small; the corresponding values for NbC are approximately ten times larger. However, in the visible range, the absorption values for SnC and NbC are of the same magnitude, with the values for NbC, being approximately two or three times larger than those for SnC and much more significant than graphene. In the ultraviolet range, the NbC optical absorption is near zero. Furthermore, SnC and graphene have similar maximum values for absorption but at different energies. Finally, the reflectivity for graphene is the largest but similar to NbC; in the case of SnC, it is near zero. In the infrared range, the inclusion of SOC generates small changes. The inclusion of SOC generates more significant changes in the visible spectrum than in the infrared region. However, for the ultraviolet region, including SOC causes more substantial changes than in the infrared and visible ranges.

Finally, including the SOC term in the reflectivity calculation generates significant changes for SnC, and NbC does not change and remains very small.

If we have doping in NbC or SnC, we expect that the electrical conductivity and the optical properties we have calculated will change; thus, we could use these materials as sensors, for example. Furthermore, we may tailor the band gap in these materials to tune the electrical conductivity, optical absorption, and reflectivity.

Author Contributions: Conceptualization, validation, formal analysis, N.D. and L.F.M.; resources, L.F.M.; data curation, investigation, methodology, E.G., O.S., N.D. and L.F.M.; writing—original draft preparation and writing—review and editing, N.D. and L.F.M.; project administration and funding acquisition, L.F.M. All authors have read and agreed to the published version of the manuscript.

Funding: This research was funded by Dirección General de Asuntos del Personal Académico de la Universidad Nacional Autónoma de México by grant IN102323.

Data Availability Statement: Not available.

Acknowledgments: We thank Dirección General de Asuntos del Personal Académico de la Universidad Nacional Autónoma de México for partial financial support by grant IN102323. We also appreciate UNAM-Miztli-Super-Computing Center's technical assistance with the project LANCAD-UNAM-DGTIC-030.

Conflicts of Interest: The authors declare no conflict of interest.

References

1. Williams, W.S. The thermal conductivity of metallic ceramics. *JOM* **1998**, *50*, 62–66. [[CrossRef](#)]
2. Zhang, B.; Huang, Y.; Bao, W.; Wang, B.; Meng, Q.; Fan, L.; Zhang, Q. Two-dimensional stable transition metal carbides (MnC and NbC) with prediction and novel functionalizations. *Phys. Chem. Chem. Phys.* **2018**, *20*, 25437–25445. [[CrossRef](#)] [[PubMed](#)]
3. Cuppari, M.G.D.V.; Santos, S.F. Physical Properties of the NbC Carbide. *Metals* **2016**, *6*, 250. [[CrossRef](#)]
4. Benzair, A.; Bouhaf, B.; Khelifa, B.; Mathieu, H.; Aourag, H. The ground state and the bonding properties of the hypothetical cubic zinc-blende-like GeC and SnC Compounds. *Phys. Lett. A* **2001**, *282*, 299–308. [[CrossRef](#)]
5. Khenata, R.; Baltache, H.; Sahnoun, M.; Driz, M.; Rérat, M.B.; Abbar, B. Full potential linearized augmented plane wave calculations of structural and electronic properties of GeC, SnC and GeSn. *Phys. B* **2003**, *336*, 321–328. [[CrossRef](#)]
6. Hoat, D.M.; Naseri, M.; Ponce-Pérez, R.; Hieu, N.N.; Rivas-Silva, J.F.; Vu, T.V.; Tong, H.D.; Cicoletzi, G.H. Structural and electronic properties of chemically functionalized SnC monolayer: A first principles study. *Mater. Res. Express* **2020**, *7*, 015013. [[CrossRef](#)]
7. Rehman, J.; Fan, X.; Zheng, W.T. 2D SnC sheet with a small strain is a promising Li host material for Li-ion batteries. *Mater. Today Commun.* **2021**, *26*, 101768. [[CrossRef](#)]
8. Butt, M.K.; Zeeshan, H.M.; Dinh, V.A.; Zhao, Y.; Wang, S.; Jin, K. Monolayer SnC as anode material for Na ion batteries. *Comput. Mater. Sci.* **2021**, *197*, 110617. [[CrossRef](#)]
9. Giannozzi, P.; Baroni, S.; Bonini, N.; Calandra, M.; Car, R.; Cavazzoni, C.; Ceresoli, D.; Chiarotti, G.L.; Cococcioni, M.; Dabo, I.; et al. QUANTUM ESPRESSO: A Modular and Open-Source Software Project for Quantum Simulations of Materials. *J. Phys. Condens. Matter* **2009**, *21*, 395502. [[CrossRef](#)] [[PubMed](#)]
10. Troullier, N.; Martins, J.L. Efficient Pseudopotentials for Plane-Wave Calculations. *Phys. Rev. B* **1991**, *43*, 1993–2006. [[CrossRef](#)] [[PubMed](#)]
11. Perdew, J.P.; Burke, K.; Ernzerhof, M. Generalized Gradient Approximation Made Simple. *Phys. Rev. Lett.* **1996**, *77*, 3865–3868. [[CrossRef](#)] [[PubMed](#)]
12. Monkhorst, H.J.; Pack, J.D. Special Points for Brillouin-Zone Integrations. *Phys. Rev. B* **1976**, *13*, 5188–5192. [[CrossRef](#)]
13. Lide, D.R. *CRC Handbook of Chemistry and Physics: A Ready-Reference Book of Chemical and Physical Data*, 81st ed.; CRC Press: Boca Raton, FL, USA, 2000; pp. 2000–2001. ISBN 978-0-8493-0481-1.
14. Kumar, S.; Maurya, T.K.; Auluck, S. Electronic and optical properties of ordered BexZn 1-xSe alloys by the FPLAPW method. *J. Phys. Condens. Matter* **2008**, *20*, 075205. [[CrossRef](#)]
15. Kittel, C. *Introduction to Solid State Physics*, 3rd ed.; John Wiley: New York, NY, USA, 1966; p. 648.
16. Salas, O.; Garcés, E.; Magana, L.F. The Interaction of the 2D MoP2 and NbP2 Surfaces with Carbon Dioxide and Carbon Monoxide and Changes in their Optical Properties. *Crystals* **2022**, *12*, 45. [[CrossRef](#)]
17. Mostofi, A.A.; Yates, J.R.; Pizzi, G.; Lee, Y.S.; Souza, I.; Vanderbilt, D.; Marzari, N. A tool for obtaining maximally-localized Wannier functions. *Comput. Phys. Commun.* **2014**, *185*, 2309. [[CrossRef](#)]
18. Pizzi, G.; Volja, D.; Kozinsky, B.; Fornari, M.; Marzari, N. Boltzmann: A code for the evaluation of thermoelectric and electronic transport properties with a maximally localized Wannier functions basis. *Comput. Phys. Commun.* **2014**, *185*, 422–429. [[CrossRef](#)]
19. Islam, M.R.; Wang, Z.; Qu, S.; Liu, K.; Wang, Z. The impact of spin-orbit coupling and the strain effect on monolayer tin carbide. *J. Comput. Electron.* **2021**, *20*, 151. [[CrossRef](#)]

Disclaimer/Publisher's Note: The statements, opinions and data contained in all publications are solely those of the individual author(s) and contributor(s) and not of MDPI and/or the editor(s). MDPI and/or the editor(s) disclaim responsibility for any injury to people or property resulting from any ideas, methods, instructions or products referred to in the content.